Demagnetization signatures of lunar impact craters

J. S. Halekas,[1] D. L. Mitchell,[1] R. P. Lin,[1] L. L. Hood,[2] M. H. Acuña,[3] and A. B. Binder[4]

Received 16 August 2001; revised 25 January 2002; accepted 25 January 2002; published 12 July 2002.

[1] We investigate the crustal magnetic signatures of lunar craters using Lunar Prospector (LP) electron reflectometer data. Craters of all ages often have associated magnetic lows, showing that crustal fields were present even in pre-Nectarian times ($\gtrsim$3.9 Ga). Magnetic lows extend to $\sim$2–4 crater radii, suggesting shock rather than thermal demagnetization. Younger craters are more likely to have clear and complete demagnetization signatures, suggesting that many older magnetic lows have been subsequently obscured. No size dependence is found for craters larger than 50 km in diameter, suggesting that demagnetization effects for all craters in this size range completely penetrate the magnetized layer. If shock demagnetization is responsible, this suggests an upper limit of $\sim$50 km for the depth of magnetization. Evidence of edge effects due to magnetization contrasts may show that strong far-side crustal fields are coherent at scales of $\sim$25 km. *INDEX TERMS:* 5440 Planetology: Solid Surface Planets: Magnetic fields and magnetism; 5420 Planetology: Solid Surface Planets: Impact phenomena (includes cratering); 6250 Planetology: Solar System Objects: Moon (1221)

1. Introduction

[2] The first measurements of lunar crustal magnetic fields were made by experiments on the Apollo subsatellites [*Anderson et al.*, 1976]. Apollo data showed [*Lin et al.*, 1988], and LP data confirmed [*Hood et al.*, 2001], that the largest regions of strong magnetic fields (>50 nT) lie on the lunar far side, diametrically opposite (antipodal) to the Orientale, Imbrium, Serenitatis, Crisium, and (to a lesser extent) Nectaris impact basins. Shock remanence generated by a combination of magnetic field amplification by plasma compression, and focussing of seismic waves and solid ejecta, may be responsible for these antipodal signatures [*Hood and Huang*, 1991]. Meanwhile, observations show that large impact basins themselves tend to have very weak fields (<0.5 nT). On smaller scales, lunar crustal fields and surface geology are so jumbled that, while it is possible to find statistical differences in the magnetism of different terranes, attempts to correlate magnetic anomalies with specific geologic terranes have met with only limited success [*Halekas et al.*, 2001; *Hood et al.*, 2001; *Russell et al.*, 1977]. However, because of the limitations of available data, few studies have focused on the weakly magnetized regions of the Moon. Mapping techniques which rely on spacecraft magnetometer measurements can only measure surface fields which are coherent and strong enough to be seen at orbital altitude. Electron reflectometry can detect very small surface fields ($\sim$0.2 nT), but careful corrections must be made for the effects of surface electrostatic charging on measurements of weak magnetic fields [*Halekas et al.*, 2001]. These corrections have now been made for the LP data, allowing us for the first time to investigate in detail the regions of low crustal magnetic fields on the lunar surface.

[3] For this study we chose to investigate the magnetic properties of lunar impact craters. The heating and shock pressures generated by large impacts are more than sufficient to erase existing magnetic remanence. Statistical results confirm that lunar impact craters and basins, especially of Imbrian age and younger, tend to have lower magnetic fields than their surroundings [*Halekas et al.*, 2001]. Furthermore, studies have found that this is also true of Martian and terrestrial impact craters [*Nimmo and Gilmore*, 2001; *Pilkington and Grieve*, 1992; *Scott et al.*, 1997].

[4] We use electron reflectometry measurements which have been corrected for electric fields and converted to estimates of surface magnetic field magnitude. The intrinsic spatial resolution of the data is several km, however at these scales we are drastically undersampled [*Halekas et al.*, 2001]. Therefore, to achieve good coverage with acceptable resolution, these measurements are binned at 0.5° resolution, and boxcar smoothed over 1.5° × 1.5°. This yields a data set with 45 km resolution at the equator. We therefore restrict our study to 557 lunar craters with diameters greater than 50 km.

2. Demagnetized Craters

[5] Figure 1 shows four magnetic profiles averaged over 90°, and a profile averaged over all angles, for the Imbrian crater Keeler (160 km diameter). A magnetic low is centered over the crater and extends to $\sim$1.5 crater radii. The magnetic signature is relatively symmetric close to the crater, as shown by the fact that, near the crater, all of the profiles correspond closely. Outside of the magnetic low they diverge as the effects of other magnetic sources dominate.

[6] We have calculated similar magnetic profiles for all 557 craters in our study group. Of these craters, $\sim$30% lie at least partly in regions in which there is no data. Of the remaining craters, many either have magnetic fields comparable to their surroundings or, even if they have lower average fields than their surroundings, do not have magnetic mimima centered over the craters. We selected 100 craters which, like Keeler, have relatively symmetric magnetic lows centered on the craters. It is important to note that these are not all of the demagnetized craters on the lunar surface, but merely those for which we can identify clearly associated symmetric demagnetization signatures. The limitations of our data set and the presence of nearby magnetic sources often prevent clear identification of such signatures, even when the average fields in the craters are weaker than the background fields. We are better able to identify demagnetization signatures in strongly magnetized regions and thus we have selected proportionally more in these regions. Other than this bias, the craters are essentially randomly distributed over the surface.

[7] The results of our selection process are shown in Table 1. The craters have been sorted by age unit (with approximate age range listed in Ga). The number of craters which have not been subsequently filled by mare basalts, light plains materials, or terra materials is shown in parentheses (as determined by geologic maps [*Lucchita*, 1978; *Scott et al.*, 1977; *Stuart-Alexander*, 1978; *Wilhelms and McCauley*, 1971; *Wilhelms and El Baz*, 1977; *Wilhelms et al.*, 1979]). The percentage of craters in each age group which

[1]Space Sciences Laboratory, University of California, Berkeley, USA.
[2]Lunar and Planetary Laboratory, University of Arizona, Tucson, USA.
[3]NASA Goddard Space Flight Center, Greenbelt, Maryland, USA.
[4]Lunar Research Institute, Tucson, Arizona, USA.

0094-8276/02/2001GL013924

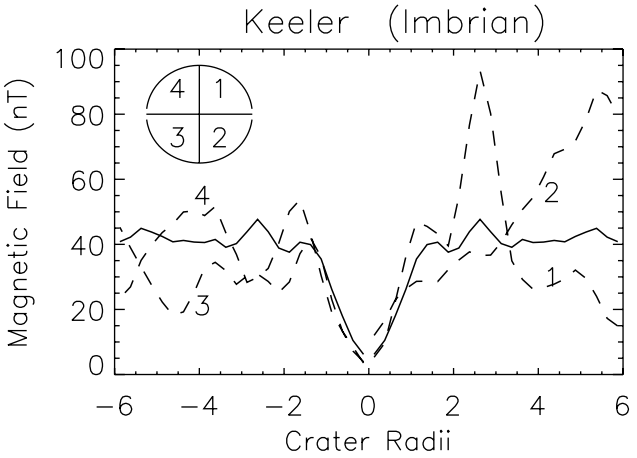

Figure 1. Magnetic properties of the 160 km diameter Imbrian crater Keeler. The solid lines show magnetic field versus distance from the crater center (normalized by crater radius), averaged over all angles. The crater has also been split into four 90° wedges as shown in the upper left, and profiles have been calculated by averaging separately over each angular range. These four profiles are shown by the four dashed lines.

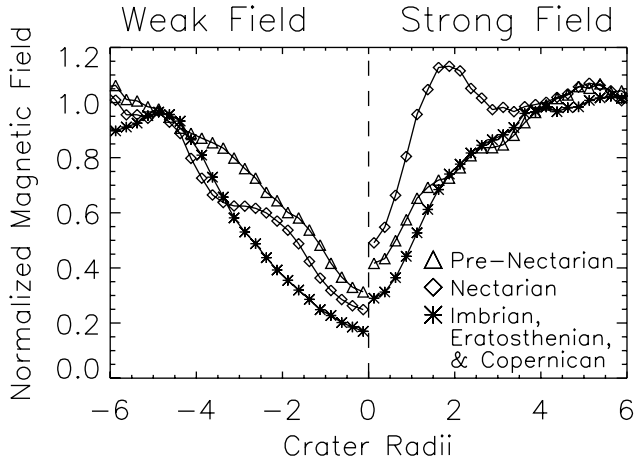

Figure 2. Average magnetic profiles of lunar craters with clear demagnetization signatures, sorted by age. Profiles are normalized by background magnetic field and crater radius. The profiles shown on the right are for craters which lie in the strongly magnetized regions within two basin radii of the antipodes of Nectaris, Crisium, Serenitatis, Imbrium, or Orientale. Those on the left are in regions outside of these. Average magnetic profiles are shown for Copernican, Eratosthenian, and Imbrian craters (18 craters in the strong-field regions, 14 in the weak-field regions), Nectarian craters (21 strong-field, 15 weak-field), and pre-Nectarian craters (12 strong-field, 20 weak-field).

have clear demagnetization signatures is also shown. The maximum of 40% reflects the limitations of our data coverage and the stringency of our selection criteria.

3. Characteristics of Demagnetization Signatures

[8] We now focus our attention on only the 100 craters which are clearly demagnetized. We separate the craters which lie within two basin radii of the antipode centers of Orientale, Imbrium, Serenitatis, Crisium, and Nectaris, thus selecting craters which lie in large regions of strong magnetic fields. This separation is meaningful because the antipodal regions may have been magnetized by the mechanism proposed by [*Hood and Huang*, 1991], while the magnetization outside of these regions may have other sources, perhaps including magnetized basin ejecta [*Halekas et al.*, 2001; *Hood et al.*, 2001].

[9] Within these two groups we sort the craters by age (Figure 2) and by size (Figure 3). It is immediately apparent from either figure that craters in the non-antipodal weak-field regions have demagnetization signatures which are wider and deeper (extending out to 4–5 crater radii, and demagnetized to 20–30% of the ambient field) than those in the antipodal strong-field regions (2–3 radii wide, and demagnetized to 30–50%).

[10] There is a slight apparent trend in demagnetization versus age, with younger craters more completely demagnetized than older ones. There is no clear trend in demagnetization versus size.

[11] There is an anomalous effect in the data for Nectarian craters and craters of 50–90 km in diameter in the strongly magnetic regions. Instead of a smoothly varying magnetic signature, these show a peak at about two crater radii. The peak is seen in 12/21 individual crater profiles in the strong-field Nectarian bin, and in 6/9 and 10/19 profiles in the 50–70 and 70–90 km diameter strong-field bins. Similar peaks are also seen in 6/12 strong-field pre-Nectarian crater profiles, but they lie at varying radii and do not add constructively. More such peaks are found in other

Table 1. Lunar Craters with Diameter >50 km

Crater Age (Ga)	Number (Unfilled)	Demagnetized (Unfilled)	Percent
Coper. (0–1)	15 (15)	6 (6)	40%
Erat. (1–3.2)	21 (21)	6 (6)	29%
Imbr. (3.2–3.8)	87 (61)	20 (12)	23%
Nect. (3.8–3.9)	177 (67)	36 (13)	20%
Pre-N. (>3.9)	267 (148)	32 (17)	12%

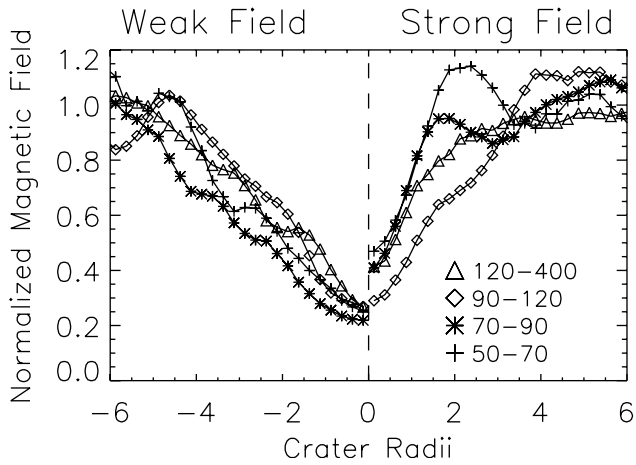

Figure 3. Average magnetic profiles of lunar craters with clear demagnetization signatures, sorted by size. Profiles are normalized by background magnetic field and crater radius. The profiles shown on the right are for craters which lie in the strongly magnetized regions within two basin radii of the antipodes of Nectaris, Crisium, Serenitatis, Imbrium, or Orientale. Those on the left are in regions outside of these. Average magnetic profiles are shown for craters with diameters between 50 and 70 km (9 craters in the strong-field regions, 11 in the weak-field regions), 70 and 90 km (19 strong-field, 12 weak-field), 90 and 120 km (8 strong-field, 11 weak-field), and 120 and 400 km (15 strong-field, 15 weak-field).

individual crater profiles, but not for more than 27% of the craters in any other age or size bin.

4. Conclusions and Implications

[12] A substantial number of lunar craters greater than 50 km in diameter (100 out of the 557 craters studied) are clearly demagnetized. Though some craters of all ages are demagnetized (showing that crustal magnetism was present before even some pre-Nectarian craters), the percentage steadily decreases with age. Furthermore, of the craters which are clearly demagnetized, there is a hint of a trend in age, with younger craters slightly more demagnetized. This suggests that older craters may have been remagnetized or subsequently overlain by magnetized materials. The second hypothesis seems unlikely to explain all of the data, since many craters without significant visible fill do not have associated magnetic lows, while many subsequently filled craters still have clear demagnetization signatures. Magnetic fill could be responsible for erasing some of the demagnetization signatures, but for it to account for all of them it would have to be thin enough to be unmapped. It therefore seems likely that at least some of the craters have been subsequently remagnetized, perhaps by cooling through the Curie point in an ambient field or by some shock related process. We do not see strong anomalies or edge effects associated with most craters, so whatever the process, it must not have produced strongly coherent magnetic fields.

[13] We find that demagnetization effects extend well beyond the main crater rims, which suggests that shock demagnetization is responsible. Thermal demagnetization requires temperatures above the Curie point (~770 deg C). Shock pressures of $\gtrsim$100 kbar are necessary to generate these postshock temperatures in lunar fines [*Ahrens and Cole*, 1974]. These shock pressures are only found well inside the crater rim. On the other hand, a number of authors have found experimental evidence that shock pressures on the order of only 10 kbar or less can remove magnetic remanence, while even a few kbar can reduce it [*Cisowski and Fuller*, 1978; *Hargraves and Perkins*, 1969; *Pohl et al.*, 1975]. Using approximate scaling laws and pressure attenuation curves [*Ahrens and O'Keefe*, 1977; *Melosh*, 1989], we estimate that an impact that would produce a 50–100 km diameter crater could produce shock pressures of 10 kbar at a distance of 1.5–2 crater radii. If shock pressures of a few kbar can at least partially demagnetize, as is suggested by experiment, then shock could produce signatures as wide as those observed.

[14] We find no clear size trend, suggesting that demagnetization effects from all of the selected craters have completely penetrated the magnetized layer of the crust. Observed demagnetization signatures are several crater radii wide, and if shock is responsible, should extend as deep, since modeled peak shock pressures attenuate with nearly spherical symmetry except in the near-surface zone [*Melosh*, 1989]. Therefore, demagnetization effects should extend to depths of ~50 km for even the smallest craters surveyed. This therefore sets an upper bound on the depth to which the crust is magnetized. This may represent the maximum depth at which significant magnetic carriers are present, or it may indicate the depth of the Curie isotherm when the magnetization was emplaced.

[15] The minimum magnetic field reached in the centers of the most demagnetized craters is, on average, ~20% of the background field. The small magnetic fields which remain may indicate that the demagnetization mechanism is not completely efficient, or they may merely be leakage fields from nearby magnetic sources.

[16] There are clear differences between the demagnetization properties of craters in the strongly magnetized antipodal regions and those outside of them. The craters in weakly magnetized regions have proportionally wider and deeper demagnetization signatures than those in strongly magnetized regions. We can only speculate that this dichotomy is due to differences in either the magnetization mechanisms or the magnetic carriers in the two regions. Since there are physical reasons to expect that the magnetization mechanisms may be different [*Hood and Huang*, 1991], this explanation may be more likely.

[17] Magnetic profiles for smaller craters, especially of Nectarian age, show peaks which, if real, may be interpreted as edge effects arising from magnetization contrasts. Forward modeling suggests that if the local magnetic coherence scale was on the order of half of the diameter of the craters (i.e. 25–35 km) then one would see edge effects like those observed resulting from the contrast between demagnetized craters and magnetized surroundings. The fact that they are seen only for the smallest craters in the strongly magnetized regions supports this interpretation, since it is difficult to imagine another mechanism which would produce such peaks for only those craters. However, it is extremely puzzling that Nectarian (and possibly pre-Nectarian) craters preferentially show this effect.

[18] The lack of edge effects for the rest of the craters surveyed constrains the coherence scale of the magnetic field to $\lesssim$25 km outside of the strongly magnetized antipodal regions. This should not be surprising, considering that in situ magnetometer measurements on the near side showed fields which varied greatly in magnitude and direction over only a few km [*Dyal et al.*, 1974].

[19] **Acknowledgments.** The authors thank two referees for many helpful and constructive comments. Research at the University of California, Berkeley, was supported by NASA through subcontract LRI-99-101 from the Lunar Research Institute.

References

Ahrens, T. J., and D. M. Cole, Shock compression and adiabatic release of lunar fines from Apollo 17, *Proc. Lunar Sci. Conf.*, *5*, 2333–2345, 1974.

Ahrens, T. J., and J. D. O'Keefe, Equations of state and impact-induced shock-wave interaction on the Moon, in *Impact and Explosion Cratering*, edited by D. J. Roddy, R. O. Pepin, and R. B. Merrill, pp. 639–656, Pergamon, New York, 1977.

Anderson, K. A., R. P. Lin, J. E. McCoy, and R. E. McGuire, Measurements of lunar and planetary magnetic fields by reflection of low energy electrons, *Space Sci. Instrum.*, *1*, 439, 1976.

Cisowski, S. M., and M. Fuller, The effect of shock on the magnetism of terrestrial rocks, *J. Geophys. Res.*, *83*, 3441–3458, 1978.

Dyal, P., C. W. Parkin, and W. D. Daily, Magnetism and the interior of the Moon, *Rev. Geophys. Space Phys.*, *12*, 568–591, 1974.

Halekas, J. S., D. L. Mitchell, R. P. Lin, S. Frey, L. L. Hood, M. H. Acuña, and A. B. Binder, Mapping of crustal magnetic anomalies on the lunar near side by the Lunar Prospector electron reflectometer, *J. Geophys. Res.*, *106*, 27,841–27,852, 2001.

Hargraves, R. B., and W. E. Perkins, Investigations of the effect of shock on natural remanent magnetism, *J. Geophys. Res.*, *74*, 2576–2589, 1969.

Hood, L. L., and Z. Huang, Formation of magnetic anomalies antipodal to lunar impact basins: Two-dimensional model calculations, *J. Geophys. Res.*, *96*, 9837–9846, 1991.

Hood, L. L., A. Zakharian, J. Halekas, D. L. Mitchell, R. P. Lin, M. H. Acuña, and A. B. Binder, Initial mapping and interpretation of lunar crustal magnetic anomalies using Lunar Prospector magnetometer data, *J. Geophys. Res.*, *106*, 27,825–27,840, 2001.

Lin, R. P., K. A. Anderson, and L. Hood, Lunar surface magnetic field concentrations antipodal to young large impact basins, *Icarus*, *74*, 529–541, 1988.

Lucchita, B. K., Geologic map of the north side of the Moon, *U.S. Geol. Surv. Misc. Geol. Inv. Map*, *I-1062*, 1978.

Melosh, H. J., *Impact Cratering: A Geologic Process*, 245 pp., Oxford Univ., New York, 1989.

Nimmo, F., and M. S. Gilmore, Constraints on the depth of magnetized crust on Mars from impact craters, *J. Geophys. Res.*, *106*, 12,315–12,323, 2001.

Pilkington, M., and R. A. F. Grieve, The geophysical signatures of terrestrial impact craters, *Rev. Geophys*, *30*, 161–181, 1992.

Pohl, J., U. Bleil, and U. Horenmann, Shock magnetization and demagnetization of basalt by transient stress up to 10 kbar, *J. Geophys.*, *41*, 23–41, 1975.

Russell, C. T., H. Weiss, P. J. Coleman, Jr., L. A. Soderblom, D. E. Stuart-Alexander, and D. E. Wilhelms, Geologic-magnetic correlations on the moon—Apollo subsatellite results, *Proc. Lunar Planet. Sci. Conf.*, *8*, 1171–1185, 1977.

Scott, D. H., J. F. McCauley, and M. N. West, Geologic map of the west side of the Moon, U.S, *Geol. Surv. Misc. Geol. Inv. Map*, *I-1034*, 1977.

Scott, R. G., M. Pilkington, and E. I. Tanczyk, Magnetic investigations of the West Hawk, Deep Bay, and Clearwater impact structures, Canada, *Meteorit. Plan. Sci.*, *32*, 293–308, 1997.

Stuart-Alexander, D. E., Geologic map of the central farside of the Moon, *U.S. Geol. Surv. Misc. Geol. Inv. Map*, *I-1047*, 1978.

Wilhelms, D. E., and F. El Baz, Geologic map of the east side of the Moon, *U.S. Geol. Surv. Misc. Geol. Inv. Map*, *I-948*, 1977.

Wilhelms, D. E., and J. F. McCauley, Geologic map of the near side of the Moon, *U.S. Geol. Surv. Misc. Geol. Inv. Map*, *I-703*, 1971.

Wilhelms, D. E., K. A. Howard, and H. G. Wilshire, Geologic map of the south side of the Moon, *U.S. Geol. Surv. Misc. Geol. Inv. Map*, *I-1162*, 1979.

J. S. Halekas, D. L. Mitchell, and R. P. Lin, Space Sciences Laboratory, University of California, Berkeley, CA 94720, USA. (jazzman@ssl.berkeley.edu)

L. L. Hood, Lunar and Planetary Laboratory, University of Arizona, Tucson, AZ 85721, USA.

M. H. Acuña, NASA Goddard Space Flight Center, Greenbelt, MD 20771, USA.

A. B. Binder, Lunar Research Institute, Tucson, AZ 85747, USA.